Chapter 4

How Propellants Burn

§ 4.0 *Introduction*

Propellants (for the purpose of this book) are energetic substances which are used to provide the energy for projectiles as discharged from guns. They are also used in providing the propulsive force for rockets. Their principal property is that they contain the oxygen required to burn and do not require to be exposed to air in order to oxidise. They are almost all compounds of nitrogen. This element has a unique property that most compounds of nitrogen are unstable, and decompose with relatively little provocation.

Historically, the earliest explosive was *black powder*, which after 800 years of trial and error, is today is a mixture of potassium nitrate (75%), sulphur (10%) and charcoal (15%), ground together into a fine powder. This 'meal' is then transformed into a cohesive conglomerate by compression into a cake, which is broken up into the required granular size. Alternatively, the meal is made into a paste with water (or alcohol). This paste is forced through a sieve to form granules, which are then dried. Black powder originates in China, possibly dating back to pre BC. By the middle of the 13th century knowledge of it had travelled to Europe, when the English monk Roger Bacon wrote down a formula in his Opus Majus in 1267. It is recorded that handguns were discharged from the walls of Stirling Castle (Scotland) in 1304, and that cannon were used at the Battle of Crecy (France) in 1346. By that time too it is known that there were a number of black powder mills in Europe. Black powder continued to be the main explosive in use in war and in peace for the next five hundred years until it was largely superseded by more efficient substances. But it has properties that still make it useful to this day as the initiator for the main charge in large guns.

Black powder is inefficient in that it does not completely decompose into gasses, and in consequence a lot of smoke is created as it burns. The average molecular weight of the final decomposition gasses is also rather high, which limits the amount of work these gasses can do pushing the projectile up the barrel compared to that of modern propellants. (See § 3.2).

In 1845, the German chemist Christian Schönbein discovered that an explosive could be made by the nitration of cellulose, which was much more energetic than black powder and was 'smokeless' since it decomposed completely into gasses. In the 1880s it was found that this *nitrocellulose* could be plasticised by dissolving it in a mixture of alcohol

and ether. This form of nitrocellulose had burning properties that made it suitable for use in guns. (Vieille, the French ballistician, is usually cited as having made this discovery in 1886. However, German literature gives the credit to Duttenhofer of the Rottweil plant, though the process was only revealed by them in 1887). During World War One, German chemists found that dissolving nitrocellulose in another explosive, *nitroglycerine*, simplified the production of gun propellants (in that the solvent did not have to be removed from the plasticised nitrocellulose) and also produced a more energetic propellant. These so-called 'double-base' propellants burned at a higher temperature than 'single-base' nitrocellulose propellants and the consequential increased erosion in gun barrels shortened their lifetime significantly. Since World War Two, another explosive, *nitroguanidine*, has increasingly been added to form a 'triple-base' propellant, which has a lower burning temperature than even single-base nitrocellulose, and so inflicts less erosion problems. However, these triple-base propellants are usually reserved for large guns and are not used in small-arms propellants.

A sophisticated technology in modifying the burning properties of these 'smokeless' propellants has been developed over the years. The use of additives and deterrents, together with the geometry of the propellant powder kernels, continues to improve the generation of high projectile muzzle energies, without the penalty of high chamber pressures and barrel erosion, which is the Holy Grail of propellant science. A full account of the production methods of propellants can be found in Hayes "Elements of Ordnance" [1] which is still instructive today despite its antiquity.

§ 4.1 *The various ways in which a propellant can burn*

There are three ways in which an explosive can 'burn'; by *combustion*, by *explosion* and by *detonation*.

Combustion occurs when the explosive burns in air, or some other source of oxygen. Most propellant nitro-powders burn quietly with little flame and no smoke.

Explosion takes place in the absence of additional oxygen. This can be a very slow process as it is actually the decomposition of the propellant, the speed of which depends (initially at any rate) on the temperature. It is a surface effect and the propellant decomposes from the outside inwards. At room temperature, the rate of decomposition of a propellant powder can be measured in years. But if the temperature is raised so that the rate of explosion increases, and it is confined so that the pressure increases, then the

decomposition can be very rapid, so that it 'explodes' in the common understanding of the term.

Detonation is an extremely violent and rapid phenomenon and is as fast again compared to the explosion process, as explosion is to combustion. The whole solid mass decomposes almost simultaneously as a detonation wave travels through the explosive at the speed of sound, which can be some thousands of feet per second. All explosives will detonate if provoked strongly enough, usually when subjected to a shock of some kind. Black powder is usually cited as the sole exception, but detonations have been reported with a fine grained black powders in certain circumstances. Many 'high' explosives only decompose by detonation. Nitrocellulose powders are designed to explode, but will detonate if sufficiently shocked. Nitroglycerine will normally detonate, but can be made to explode by binding it with nitrocellulose.

§ 4.2 *The decomposition products of black powder*

The decomposition of black powder is a complex process. A number of stoichiometries are possible [2] and the process would seem to be sensitive to the purity and composition of the charcoal [3]. Also, black powder propellant is a mixture of potassium nitrate, sulphur and charcoal, which are not combined in a single chemical molecule containing both the fuel and the oxidant, as is the case with most modern propellants. The performance of black powder depends strongly on how finely the constituents are ground and then compressed together to form an intimate mixture at the molecular level. Trying to represent the black powder decomposition as a simple reaction proves unsatisfactory. For example, one often cited simple reaction path is,

$$S + 2KNO_3 + 3C \rightarrow K_2S + 3CO_2 + N_2$$

The atomic weights of the various elements involved are; K = 39, S = 32, O = 16, N = 14 and C = 12. The ratio by weight of the various constituents on the left hand side of this reaction path are potassium nitrate (75%), sulphur (12%) and charcoal (13%), which are reasonably close to the modern black powder constituent ratios given above.

The high pressure gasses drive the projectile up the barrel. The reaction product potassium sulphide is a black solid. For the gasses that remain, there are four molecules with a total molecular weight of 160, so the average molecular weight of the black powder gas products is 40.

The adiabatic flame temperature of black powder is measured to be about 1050°K [7]. The Force F of black powder may be estimated from $F = R T_0 / M$ (see §3.5.3). The universal gas constant R = 33386.18 psi in^3 lb^{-1} $°K^{-1}$ and so the Force will be 8.76 x 10^5 in-lb per lb. Experience would indicate that this is rather low.

The decomposition would actually appear to take place in a number of stages and the stoichiometry below has been proposed by Campbell and Weingarten [4], whereby an in initial reaction takes place between the sulphur and the potassium nitrate.

$$S + 2KNO_3 \rightarrow K_2SO_4 + 2NO$$

This reaction is sufficiently exothermic that enough heat is provided to promote the reaction by which the charcoal is burnt.

$$3C + 2KNO_3 \rightarrow K_2CO_3 + N_2 + CO_2 + CO$$

The initial reaction above was also proposed by Blackwood and Bowden [5], but they proposed different secondary reaction paths.

The white solids potassium sulphate and potassium carbonate form 'fouling' on the inside surface of the barrel, and are emitted as white smoke.

The mass ratios of the various constituents for this reaction path are potassium nitrate (86%), sulphur (7%) and charcoal (7%), which is somewhat distant from the formula given above, and which has proved efficient after many centuries of evolution. It is evident then that this also is a highly simplified description and that there must be a number of other reaction paths whose significance depends on a number of complex factors, including how well the constituents are combined so that they make intimate contact at a molecular level. This is probably one of the main reaction paths, though, so it is worth examining in a little more detail.

It can be easily deduced that the solid potassium salts constitute about 66% by weight of the explosion products of black powder from the equations above, but this is an over-estimate [6]

For the gas products, there are five molecules with a total molecular weight of 160, so the average molecular weight of the black powder gas products for this reaction path is a more reasonable 32. The Force will then be 1.1 x 10^6 in-lb per lb. This is in fair agreement with Freedman [8].

The chemical energy density of black powder would appear to vary widely depending on the purity and proportions of the various ingredients, but Freedman gives a value of 5 x 10^6 in-lb per lb. and a ratio of specific heats $\gamma = 1.22$. The chemical energy density Q is related to the Force by $F = Q(\gamma - 1)$ and the Force so derived agrees well with the value given above.

§ 4.3 *The decomposition products of nitrocellulose*

One formula for nitrocellulose, and its explosion products [9], is as follows:

$$C_{24}H_{30}O_{20}(NO_2)_{10} \rightarrow 14.11CO_2 + 9.89CO + 1.89H_2O + 13.11H_2 + 5N_2$$

All the explosion products are gasses. The average molecular weight of the gas mixture, is obtained by adding up all the atomic weights on the left hand side of the equation, which comes to 1098, and dividing by 44, the number of molecules listed on the products side of the equation, to give an average molecular weight of 25. The actual average molecular weight of nitrocellulose propellant gasses is about 23.5, so this is a reasonable approximation.

The adiabatic flame temperature of nitrocellulose propellant is about 2700˚K. The chemical energy density of nitrocellulose propellant is about 14.5 x 10^6 in-lb per lb. With this information it is possible to derive a value for the Force F = 3.6 x 10^6 in-lb per lb, and a consequent ratio of specific heats $\gamma = 1.25$. These are very reasonable approximations for nitrocellulose propellants.

§ 4.4 *The burning mechanics of explosion*

In 1839, Piobert [10] postulated that, "…. burning takes place by parallel layers, where the surface of the grain regresses, layer by layer, normal to the surface at every point."

The rate at which this regression takes place is a function of temperature, though once the ignition temperature is reached, the burning rate is strongly coupled to the pressure of the gasses surrounding the solid propellant.

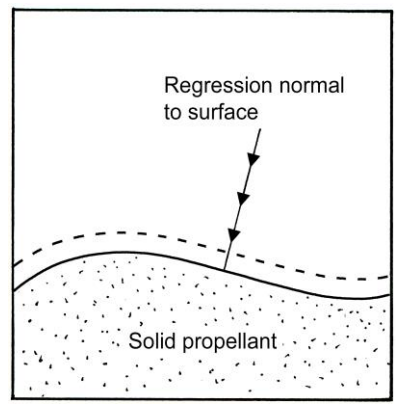

Fig. 4.1 *Propellants burn in layers normal to the surface*

In 1893, Vieile proposed [11] that De Saint-Robert's earlier assertion [12] that the rate of regression was strongly coupled to (and a simple function of) the gas pressure, did not apply to black powder as had been suggested, but did apply to plasticised nitrocellulose propellants. The relationship given by De Saint-Robert is,

$$\frac{dy}{dt} = \beta P^{\alpha} \qquad 4.1$$

where y is a direction normal to the surface of the solid propellant, P is the gas pressure and β is a *burning rate coefficient*. This is usually called Vieille's law though as noted, he was not its originator. There was much debate into the early 20th century on what value the pressure exponent α should take, but it was eventually agreed that for the pressures of interest in guns, setting $\alpha = 1$ appeared to work very well (for nitrocellulose propellants) and greatly simplified the problem of creating a closed form analytic internal ballistics model.

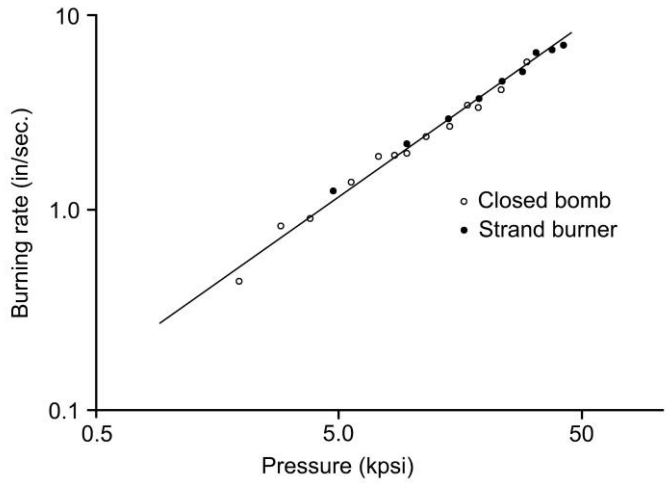

Fig. 4.2 *The burning rate (rate of regression) of military propellant M17 (from* [13]*) showing how a linear burning rate with pressure is a very reasonable approximation.*

The actual thermochemistry of burning propellants is extremely complex and while it has been studied extensively (see, for example [14]) for the comparatively low pressures at which rocket propellants operate (a few hundred psi) it is clear that the mechanisms and reactions in play at these pressures do not accurately represent the burning of propellants at the working pressures of guns (tens of thousands of psi) [15].

A highly simplified description of the actual burning dynamics is that the boiling liquid surface of the solid propellant gives off propellant gasses, which exist as a thin layer above the solid propellant, and in which some initial reactions take place. Above this layer the gasses burn luminously in an exothermic reaction, during which the final reaction products are determined. The thickness of the layer of propellant gasses depends on the gas pressure - the higher the pressure, the closer the burning layer is pushed towards the surface of the propellant. This increases the heat absorbed by the propellant surface, which occurs mainly by conduction through the unburnt gas layer. The consequence is a more vigorous boiling of the propellant gasses off the surface, thereby increasing the rate of regression. The heat conductivity of the solid propellant is very poor, so the decomposition of the solid propellant is confined to the surface. The relationship between the rate at which propellent boils off the surface and the gas pressure is almost linear once the pressure exceeds about 12,000 psi.

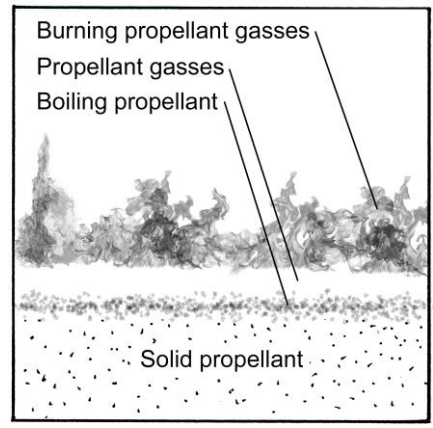

Fig. 4.3 *Progression from solid propellant to burnt propellant gasses*

§ 4.5 *Using a manometric or closed bomb to determine propellant properties*

The measurement of propellant burning properties using a *manometric bomb*, otherwise known as a *closed bomb*, has a long and illustrious history. Although other means of measuring powder burning rates more directly are available today, such as the *strand burner*, the closed bomb is still used as a principal means of determining powder burning properties.

The closed bomb is a very simple device. It is a steel container, usually a cylinder having thick walls to contain pressures of the same order as the peak pressure in guns. It has some means of igniting the charge of propellant, some means of measuring the pressure within, some means of safely bleeding off the high pressure gasses after it has been fired and, of course, there must be access to load a fresh charge of propellant.

Fig. 4.4 is a schematic of a closed bomb. In this example, a thick walled steel cylinder has plugs at each end, which can be unscrewed. Copper or bronze sealing rings (not shown)

are needed to ensure the plugs do not leak at the high pressures the vessel will need to contain. There can also be a thin walled liner tube in the chamber, which can be an insulator to reduce heat loss to the walls, or simply a sacrificial liner to be replaced when it becomes heavily eroded.

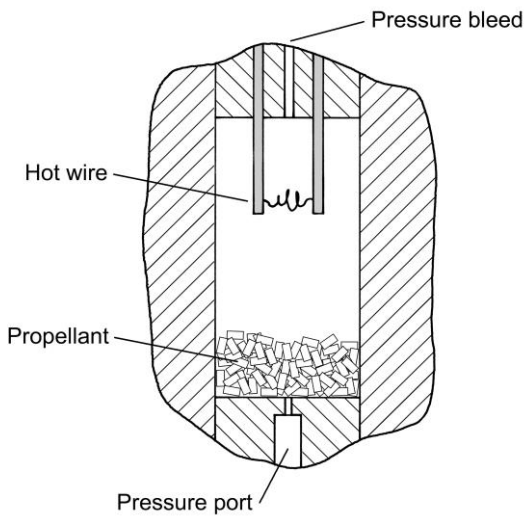

Fig. 4.4 *Schematic of a closed bomb for measuring propellant properties*

As shown, the top plug contains a small diameter hole through which the high pressure gasses could be released via a high pressure valve after the bomb is fired. This hole could also be used to introduce a flammable gas to initiate the explosion of the propellant. The gas is ignited by passing an electric current through the 'hot wire'. The bottom plug contains a pressure port into which a pressure transducer can be screwed to measure the pressure-time history as the propellant explodes within the chamber.

A detailed description of a closed bomb device is given by Hunt [16]. While this description is dated, the only real changes in the intervening seventy years is in the signal recording apparatus rather than the instrumentation itself – which, as described, would look remarkably familiar today.

It has been long appreciated that the ratio of height to width of the chamber in a closed bomb should not exceed 2 : 1 or the possibility of travelling pressure waves building up between the ends of the chamber become unacceptable. A spherical chamber would

appear to be the most ideal shape, even if it is more mechanically difficult to realise than a simple cylinder. See, for example, [17].

§ 4.5.1 *Using a closed bomb to measure propellant Force and covolume*

Prior to the turn of the 20th century, when Petavel devised his 'spring gauge' [18], which enabled the pressure in a closed bomb to be accurately recorded as a function of time, a copper crusher gauge was used to simply measure the peak pressure of the explosion gasses in the chamber. This was sufficient to be able to determine the Force of the propellant and the covolume. By extension the adiabatic burning temperature of the propellant could be determined, and the ratio of specific heats.

These parameters were sufficient to enable a theoretical description of the internal ballistics of a gun, provided certain well founded assumptions were made regarding the way propellant powder kernels burnt as a function of their shape. Petavel's spring gauge, and later J. J. Thomson's piezoelectric pressure transducer, first used in 1917 and still the main pressure measuring device used today, enabled an experimental determination of the speed at which the propellant burnt.

Recall from § 3.5.3 that the propellant Force F can be written as $F = RT_0/M$ where R is the universal gas constant, T_0 is the temperature at which the propellant burns and M is the average molecular weight of the propellant gasses. The Nobel-Abel gas equation can then be written,

$$P\left(V - m\eta\right) = mF \tag{4.1}$$

where η is the covolume of the propellant gas molecules, V is the volume of the closed bomb chamber and m is the mass of the propellant within the chamber.

It is convenient to define the *loading density* Δ as the density of propellant within the volume of the closed bomb. (Other writers give different definitions of loading density, but this is the definition used here.)

$$\Delta = \frac{m}{V} \tag{4.2}$$

Then the Nobel-Abel equation can be written as a linear equation such that,

$$\frac{P}{\Delta} = \eta P + F \tag{4.3}$$

The closed bomb can now be fired at a number of different loading densities (different charge weights of propellant) and the values of P/Δ then plotted against P. See Fig. 4.5.

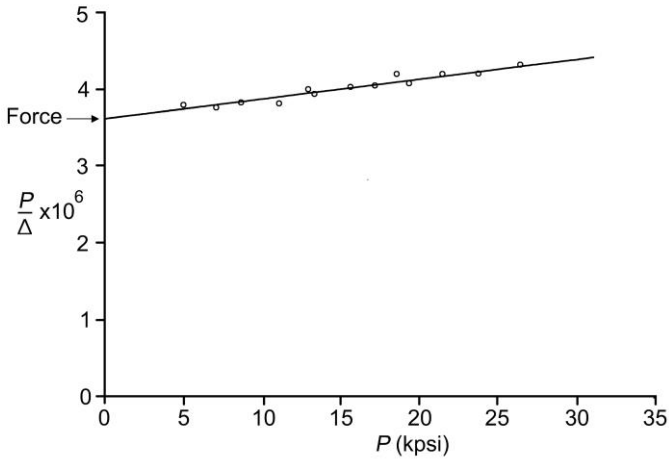

Fig. 4.5 *Plot of pressure over loading density against pressure. The intercept of a straight line fit through the vertical axis is the Force. The slope of the straight line fit is the covolume.*

The plot in Fig. 4.5 is representative for single base nitro propellants. Loading densities usually used in closed bomb tests are between 0.0018 lb/in^3 and 0.0072 lb/in^3. The density of the propellant is about 0.0584 lb/in^3, so even at the highest pressures indicated the propellant would not take up more than 15% of the volume of the closed bomb chamber. (The bulk density of small arms propellant powders is about 0.0338 lb/in^3, so the propellant powder would actually have taken up about a third of the volume of the chamber.) Loading densities of less than 2% are not suitable as the burn times of the propellant is then so long, due to the low pressures, that there is excessive heat loss to the chamber walls which lowers the pressure yet more.

A straight line fit through the data points intercepts the vertical axis at about 3650000 in-lb/lb, which is typical of the Force for single base nitro propellants. The slope of the straight line is η the covolume, which is about 25.5 in^3/lb for nitrocellulose propellant gasses. Of course, the two unknowns η and F in Eqn. 4.3 can be determined analytically by the simultaneous solution of this equation for two pressures P, rather than graphically as shown here.

It is assumed that the temperature of the propellant gasses will be T_0 the flame temperature of the burning propellant. This is called the adiabatic temperature of the gasses as this would be the temperature if there is no heat loss to the walls of the chamber.

The temperature of such a transient event is difficult to measure [19]. However, with the Force F found experimentally, and using the average molecular weight M derived from the stoichiometry, the temperature of the propellant gasses can be accurately calculated.

$$T_0 = \frac{FM}{R} \tag{4.4}$$

Using the Force F = 365000 in-lb/lb, the average molecular weight 25 determined above, and the universal gas constant R = 33386 psi in^3 lb^{-1} $^\circ K^{-1}$, the temperature can be calculated to be 2733 $^\circ$K.

The energy content or chemical energy density Q of the propellant can be found experimentally by burning a known amount of the propellant in a *calorimetric bomb*. Calorimetric bombs are used very widely outside of ballistics for measuring the energy content of many substances, including the calorie content of food. Essentially, it is a pressure vessel with a screw top through which an insulated wire is introduced for propellant ignition. The vessel has a thinner walls than the manometric bomb described above as it does not need to contain the very high pressures at which that device is required to work. The vessel is immersed in water, within a very well insulated container. When the propellant is ignited and burnt, the heat from the hot propellant gasses heats up the water surrounding the vessel. The rise in temperature of the water is measured with a thermometer. The amount of water is known, the heat capacity of water is known, so the amount of energy released by burning the propellant can be determined.

With the energy content of the propellant measured in a calorimetric bomb, and the Force of the propellant measured in a manometric bomb, the ratio of specific heats γ can be calculated from,

$$\gamma = \frac{F}{Q} + 1 \tag{4.5}$$

Typically, for single base nitrocellulose propellants, Q = 1460000 in-lb/lb so that γ = 1.25

Just using the corrected peak pressures from a copper crusher then, it is possible to determine all the main thermodynamic parameters required for a good quantitative understanding of the internal ballistics processes in a gun.

§ 4.5.2 *Corrections for energy losses*

The assumption above has been that there are no heat losses to the chamber walls or other energy losses in the closed bomb. In fact, there are a number of losses which need to be accounted for to a greater or lesser extent. Leakage of high pressure gasses due to the inadequacy of seals is always a problem in manometric bombs. Expansion of the vessel due to the high pressure gasses contained needs to be considered, as the volume at high pressures may be significantly larger than the volume at low pressures. And finally, there is the heat conduction to the walls of the chamber, which can cool the gasses significantly, so lowering the pressure.

Heat losses in closed bombs was first examined in detail by Crowe and Grimshaw in 1931 [20]. There is a continuing interest in the problem of heat losses in closed bombs, see for example [21], [22] and [23].

Heat loss will go as the area of the chamber wall. The larger the wall area, the greater the heat loss. However, the relative heat loss will depend on the size of the bomb. As the chamber wall area will go as $V^{2/3}$ it will be appreciated that for a given loading density, heat loss becomes relatively less as the size of the bomb chamber is increased. Corner [24] proposed that a reduction in pressure δP would go as,

$$\delta P \propto \frac{S}{V} t^{\frac{1}{4}} \qquad 4.6$$

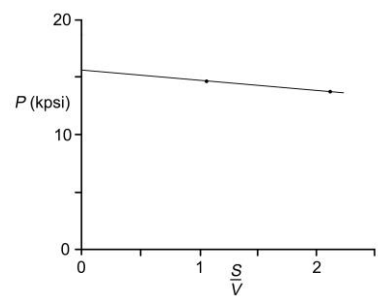

Fig. 4.6 *Plot of pressures for the same loading density in different size bombs, where the ratio S/V for one bomb is about twice that for the other.*

where S is area of the chamber wall and t is the propellant burn time. Crow and Grimshaw [op. cit] showed that where the loading density was the same, the propellant burn time was independent of the size of the closed bomb chamber. This leads to a simple experimental means of correcting for heat loss by using (at least) two bombs with different size chambers such that there is a significant difference in the ratios of S/V. The two bombs are then fired with the same loading density. A graph of peak pressure against S/V is plotted for a given loading density. A straight line is fitted to the experimental points and

extrapolated back to the vertical axis, where $S/V = 0$. This represents a bomb with zero surface area and so no heat loss. The pressures in Fig. 4.3 would then be the experimental pressures correct for heat loss in this manner.

§ 4.6 *Amount of propellant burnt and propellant gas produced*

Vieill's law (Eqn. 4.1) give the rate of regression of the propellant surface as it burns.

$$\frac{dy}{dt} = \beta P^{\alpha} \qquad 4.1$$

The parameter needed in ballistics systems - both analytic and numerical – to determine pressures and projectile velocities at any time, is the mass of propellant gas produced at any given time and this will be a function of the rate of regression.

Let C be the mass of the initial propellant charge and ρ be the density of the propellant. Then the rate at which propellant is converted to gas is a function of the surface area of the burning propellant,

$$\frac{d\mathrm{C}}{dt} = \mathrm{Area}\,\rho\,\beta\,P^{\alpha} \qquad 4.7$$

Let Z be the fraction of propellant that has burnt, such that Z = 0 before the propellant starts to burn and Z = 1 at all-burnt. Let the surface area of the burning propellant also be a function of Z. The amount of propellant burnt at any given time is C Z and so,

$$\mathrm{C}\,\frac{d\mathrm{Z}}{dt} = \mathrm{Area}_{\mathrm{Z}}\,\rho\,\beta\,P^{\alpha} \qquad 4.8$$

The charge mass C is the density ρ times the initial volume of the propellant.

$$\frac{d\mathrm{Z}}{dt} = \frac{\mathrm{Area}_{\mathrm{Z}}\,\beta\,P^{\alpha}}{\mathrm{Volume}} \qquad 4.9$$

It is convenient to assume all the kernels of propellant start burning at the same time and burn together at an equal rate. The Area and Volume in Eqn. 4.9 can then be the area and volume of one propellant kernel and their ratio is representative of the whole propellant charge at any given time.

§ 4.7 *Form factor*

Propellant powder kernels are made in a limited set of geometric shapes, dependent on the requirements of the gun in which they are to be used. They are spherical ball, cylinder (rod), flake, tube (cylinder with one hole, or perforation, through the middle) and multi-perforation cylinders. See Fig. 4.7.

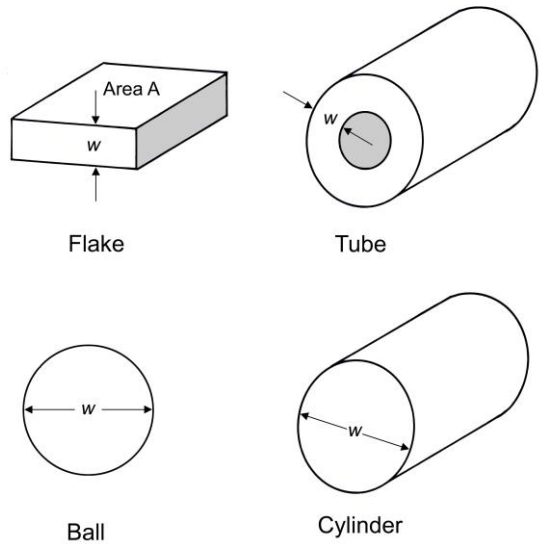

Fig. 4.7 *Four common shapes of propellant kernel*

There are variations on these themes, such as flattened ball, which burns more like a flake powder; various kinds of flake which can be round (pancake), or rectangular, or in the form of a ribbon; and randomly shaped kernels such as is the case with black powder, which are usually approximated to be spherical ball.

From geometric considerations then, it is possible to relate the area of the kernel to the volume, and so to Z, assuming the surface of the kernel deflagrates according to Vieill's Law as given in Eqn. 4.1. A 'form factor' f_Z can be defined which relates the area of the kernel for any given Z to the original area of the kernel such that,

$$\text{Area}_Z = f_Z \, \text{Area}$$

Eqn. 4.9 can be rewritten as,

$$\frac{dZ}{dt} = \frac{f_Z \,\text{Area}\,\beta\, P^{\alpha}}{\text{Volume}} \qquad 4.10$$

Z, the fraction of propellant burnt, may be expressed as,

$$Z = \frac{\text{Volume} - \text{Volume}_Z}{\text{Volume}} \quad \rightarrow \quad 1 - \frac{\text{Volume}_Z}{\text{Volume}} \qquad 4.11$$

Considering the spherical ball kernel shape, let r be the radius of the unburnt kernel and r_Z the radius after a fraction Z of the kernel has burnt. Then Eqn. 4.11 can be written,

$$Z = 1 - \frac{{}^{4}\!/_{3}\,\pi r_Z^{\,3}}{{}^{4}\!/_{3}\,\pi r^{3}} \qquad 4.12$$

Now, $\text{Area} = 4\pi r^2$ and $\text{Area}_Z = 4\pi r_Z^{\,2}$ so Eqn. 4.12 can be written as,

$$Z = 1 - \frac{\text{Area}_Z}{\text{Area}}\left(\frac{r_Z}{r}\right) \quad \rightarrow \quad 1 - \frac{\text{Area}_Z}{\text{Area}}\left(\frac{\text{Area}_Z}{\text{Area}}\right)^{\frac{1}{2}} \quad \rightarrow \quad 1 - \left(\frac{\text{Area}_Z}{\text{Area}}\right)^{\frac{3}{2}} \qquad 4.13$$

Finally then,

$$\frac{\text{Area}_Z}{\text{Area}} = \left(1 - Z\right)^{\frac{2}{3}} \quad \text{and so} \quad f_Z = \left(1 - Z\right)^{\frac{2}{3}}$$

$\dfrac{\text{Area}}{\text{Volume}}$ is just $\dfrac{4\pi r^2}{{}^{4}\!/_{3}\,\pi r^{3}} \rightarrow \dfrac{6}{w}$ where the initial radius $r = \dfrac{w}{2}$

So Eqn. 4.10 can be written as $\dfrac{dZ}{dt} = \dfrac{6\left(1 - Z\right)^{\frac{2}{2}}\,\beta\, P^{\alpha}}{w}$ 4.14

Considering a cylinder kernel and using similar arguments (with the assumption that the kernel is long compared to its diameter so that burning at the ends may be neglected), then $f_Z = \left(1 - Z\right)^{\frac{1}{2}}$ and,

$$\frac{dZ}{dt} = \frac{4\left(1 - Z\right)^{\frac{1}{2}}\,\beta\, P^{\alpha}}{w} \qquad 4.15$$

For a tube kernel (cylinder with one perforation), let r_1 is the radius of the hole or perforation through the kernel, r_2 is the outer radius of the kernel and L is the length of

the kernel. Assume that length L is long compared to the radius r_2 so that the burning of the ends may be neglected, then the area of the unburnt kernel is $2\pi \mathrm{L}\left(r_1 + r_2\right)$. When the kernel is burning, let the amount of regression be y_Z such that the area of the kernel for a given Z is $2\pi \mathrm{L}\left[\left(r_1 + y_Z\right) + \left(r_2 - y_Z\right)\right]$. Then,

$$f_Z = \frac{\mathrm{Area}_Z}{\mathrm{Area}} = \frac{2\pi \mathrm{L}\left[\left(r_1 + y_Z\right) + \left(r_2 - y_Z\right)\right]}{2\pi \mathrm{L}\left(r_1 + r_2\right)} = 1 \qquad 4.16$$

For the Area over the Volume in Eqn. 4.10,

$$\frac{\mathrm{Area}}{\mathrm{Volume}} = \frac{2\pi \mathrm{L}(r_2 + r_1)}{\pi \mathrm{L}(r_2^2 - r_1^2)} = \frac{2\pi \mathrm{L}(r_2 + r_1)}{\pi \mathrm{L}(r_2 - r_1)(r_2 + r_1)} = \frac{2}{(r_2 - r_1)} = \frac{2}{w} \qquad 4.17$$

and so Eqn. 4.10 for a tube kernel is, $\dfrac{dZ}{dt} = \dfrac{2\beta P^{\alpha}}{w}$ 4.18

Considering the flake kernel, assume that the area of the sides of the flake are small compared to the area of the top and the bottom, then a reasonable approximation is that the burning area of the kernel consists of just the top and bottom of the kernel and the burning area will remain constant from the start to the finish of the burning history of the kernel. Since the kernel is burning on both the top and the bottom surface, the ratio of the area to the volume of the kernel will go as,

$$\frac{\mathrm{Area}}{\mathrm{Volume}} = \frac{2\mathrm{A}}{\mathrm{Volume}} = \frac{2}{w} \qquad 4.19$$

and so Eqn. 4.10 can be written as, $\dfrac{dZ}{dt} = \dfrac{2\beta P^{\alpha}}{w}$ 4.20

The thickness *w* above is called the *web thickness* and is an important ballistic parameter in propellant kernel geometry. Generally, the web thickness is the shortest distance between two burning surfaces on the propellant kernel and defines the time for which the propellant kernel burns. The smaller the web thickness, the less time it takes for the propellant to be burnt up and the higher the rate at which the propellant mass is turned into propellant gasses.

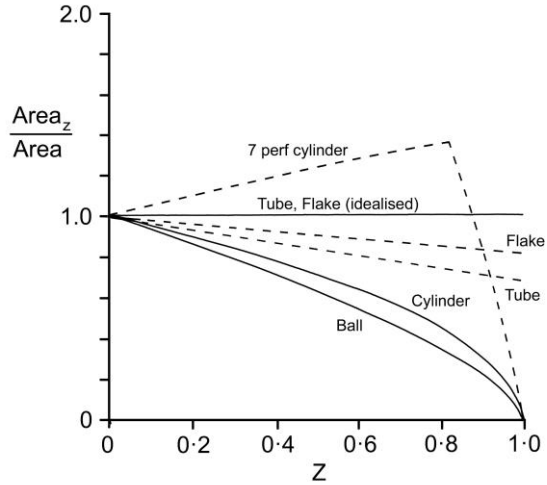

Fig. 4.8 *The change in area of a propellant kernel as it burns, relative to the area of an unburnt kernel, for various shapes of propellant kernel. The solid black lines are for the idealised functions for f_Z derived above and the dotted lines are for real kernels where the web thickness is not small compared to the kernel length and burning at the ends of the kernel is taken into account.*

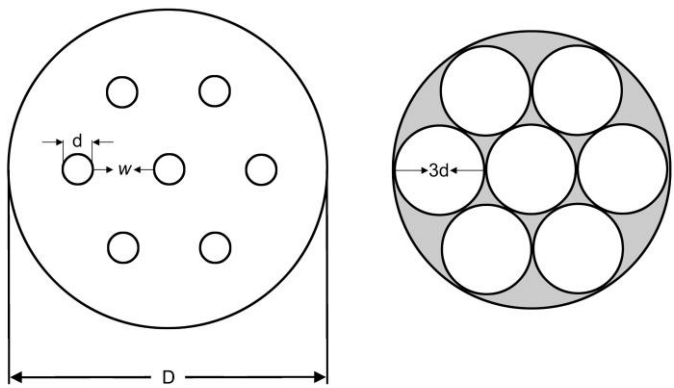

Fig. 4.9 *The left hand sketch shows a cylinder propellant kernel with seven perforations. The web thickness here is twice the diameter of the perforation. The kernel burns until the perforation diameter increases three-fold (right hand sketch), at which point it disintegrates into slivers.*

Fig. 4.8 shows how the area of the propellant kernel changes as the propellant burns for the various shapes of propellant kernel.

Propellant kernels which nominally do not change in area as they burn (tube and flake) are described as having a *neutral* shape. Where the area decreases as the kernel burns (ball, cylinder) it has a *digressive* shape. Multi-perforated cylinders are a common shape used for artillery propellant kernels and these have the property that the area actually increases as the kernel burns. Such kernels have a *progressive* shape.

The dotted line flake example is a ribbon which has thickness w, width $10w$ and a length $100w$. The dotted line tube example shown has a perforation diameter one 10^{th} the diameter of the kernel and the kernel length is the same as the diameter. In these examples, the web thickness w is not 'small' compared to the other kernel dimensions. The burning area decreases as the kernel burns and so they are actually slightly digressive.

The example of a multi-perforated cylinder shown in Fig. 4.8 is a cylinder with seven perforations. The distance between perforations is w and the perforation diameter is $0.5w$. The length of the kernel is 2.5 times the diameter D and the diameter $D = 5.5w$. See Fig. 4.9. For this particular geometry. The kernel burns progressively until the point where the walls dividing the perforations are burnt through when $Z = 0.85$. At this point, the burning area has increased 37% and so the rate of gas production has increased by 37% compared to when the kernel started burning. After this point, the slivers burn in an increasingly divergent fashion until all-burnt is reached.

The form functions described above are idealised approximations for kernel shapes that are used commonly for propellant powders, in that the web thickness is assumed to be small compared to the other dimensions of the kernel. Charbonnier [25] noted that the form function f_Z could be generalised such that,

$$f_Z = \left(1 - Z\right)^X \qquad 4.21$$

where the exponent X could be adjusted to accommodate more realistic powder kernel shapes. Table 4.1 gives the exponent X so that f_Z is a reasonable fit to the geometric fractional area change with Z for a few common real kernel shapes. In general, X is positive for digressive powder kernel shapes and X is negative for progressive powder kernel shapes.

Table 4.1 *Exponent for a number of different kernel shapes*

Kernel geometry	Exponent X
Ball	2/3
Cylinder, rod or chord (length is long compared to w)	1/2
Tube, flake, ribbon (other dimensions are long compared to w)	0
Flake (width is 10w, length is 100w)	0.1
Tube (perf is 0.1w, length is w)	0.18
7 perf cylinder (perf is 0.5w, diameter is 5.5w, length is 13.75w)	-0.22 (Z < 0.85)

More complex analytical forms are often used to describe the change in kernel area with Z. See Hunt [26], for example, for a full description. However, it is arguable that analytical forms based on geometry are not very useful today due to the widespread use of deterrents which are used to reduce the burning rate of the outer layers of the kernel. Deterrents enable propellants to burn in a more progressive manner than their geometry would indicate.

Fig. 4.10 shows a numerical simulation for three firing of a gun using the same load of the same propellant, but with three different kernel shapes: ball, tube and multi-perf. The tube shape is as described above, with a perforation one 10^{th} the diameter of the kernel, and where the length is the same as the diameter. The multi-perf shape is the seven perforation kernel described above. The kernel sizes were adjusted so that the muzzle velocity was the same in each case.

The ball shaped kernel produced the highest chamber pressure and the lowest muzzle pressure. Its digressive shape means gas production was fastest in the initial part of the projectile's journey down the barrel, which is where most of the work was done to accelerate the projectile down the barrel.

The progressive seven perf cylinder shape produced the lowest maximum chamber pressure and had a slower rise time to maximum pressure. The burning area, and so gas production, is relatively low when the free space behind the projectile is small and the projectile is moving relatively slowly up the barrel. As the projectile accelerates and the volume is increasing quickly, the burning area and so gas production increases and so pressure behind the projectile was maintained. The discontinuity at about 0.6 msec. is due to the sudden change in gas production after Z = 0.85 as the kernel disintegrates into slivers. This discontinuity is not observed in real life, however as in practice slivering is spread over time and not confined to a discrete moment. Also, slivering of multi-perf cylinder shapes seems to occur significantly earlier than would be predicted on geometric grounds. This would appear to be due to gas pressure inside the perforations breaking up the kernel as the walls between perforations become thin and fragile.

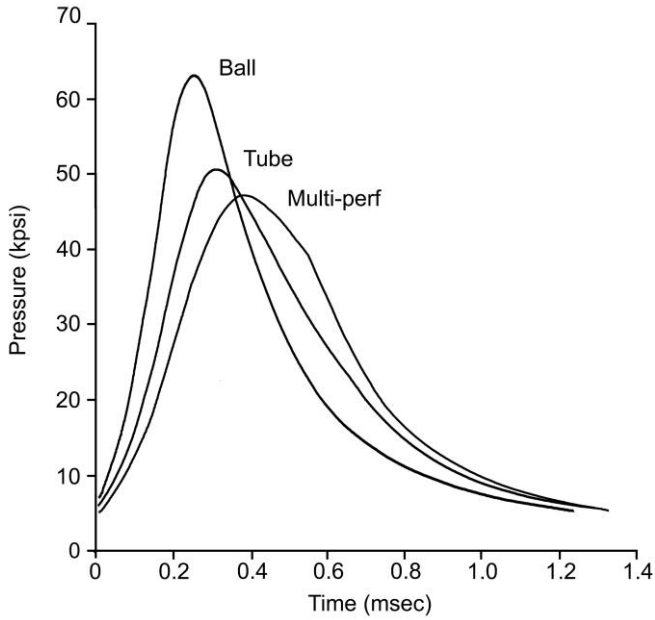

Fig. 4.10 *A numerical simulation for three firings, each with the same charge of propellant powder, each using the same propellant, but with three different kernel shapes: ball, tube and cylinder with seven perforations. The kernel sizes were adjusted so that the muzzle velocity in each case was the same.*

The performance of the nominally neutral tube shape powder was in between that of the digressive ball and the progressive multi-perf powder

§ 4.8 *Burning rate measurements*

Measuring burning rates requires a pressure measuring device whose response time is small compared to the rates of pressure change to be measured. It was not until the turn of the 20th century that Petavel started developing his eponymous spring gauge [27], which would for the first time allow accurate measurements of the pressure excursions in a closed bomb. The Petavel spring gauge had a response time of the order of 150 microseconds, which was much faster than any pressure rise time in a closed bomb.

By the 1920s, piezo-electric quartz transducers had been developed whose response time was of the order of 60 microseconds, and which could be used in guns as well as closed

bombs. But whereas the spring gauge could be calibrated by a simple apparatus involving a static weight, the piezo-electric transducer had to be calibrated by a dynamic application of pressure and this meant that the Petavel spring gauge and its successors* were regarded as more accurate than piezo-electric transducers until at least the middle of the 20th century.

As is the nature of high impedance devices, piezo-electric transducers are susceptible to transient 'ringing' which distorts their response to what are essentially step-function events. There was a dalliance with pressure gauges based around the strain gauge in the 1940s and 1950s, which could be made with a much faster response time and where transient 'ringing' was not a problem due to their low impedance. Devices based on the strain gauge were also difficult to make.

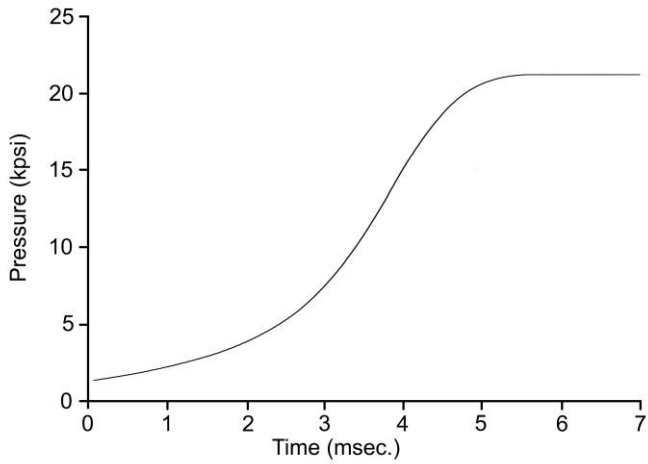

Fig. 4.8 *Pressure-time curve for a firing in a closed bomb. This was for propellant type NKT-490-B with a tube kernel geometry having length 0.050", outer diameter 0.050" and perf diameter 0.005". The kernel surface was diffused with a deterrent for more progressive burning.*

*Petavel's design was further developed by Thring and his gauge is described in the Textbook for Small Arms [28]. Interestingly, a very similar spring gauge was developed in the United States by Webster and Thompson in 1919 [29]. This was apparently an independent development as Petavel's gauge is not mentioned, but it does not seem to have been adopted in the United States with the enthusiasm that Petavel's gauge was in the United Kingdom. The German ballistician E. M. Schmitz also developed a spring gauge at the Krupp works in 1913 [30].

By the 1950s piezo-electric transducers started to become commercially available. This freed ballistics laboratories from the need for highly skilled technicians to fabricate their own pressure measuring systems. Piezo-electric transducers thus became the principal means of recording the pressure history in closed bombs and in guns, which is true to this day.

A typical pressure vs time curve for a closed bomb firing is shown in Fig. 4.8. Once the pressure has reached a peak, it starts to decay due to heat loss to the walls of the chamber, but this decay period is usually long compared to the risetime to peak pressure. It is a reasonable argument that correcting for heat loss is "an optional extra". However, The heat loss at peak pressure can be determined experimentally as in § 4.5.2 and then applied proportionately to all pressures along the curve.

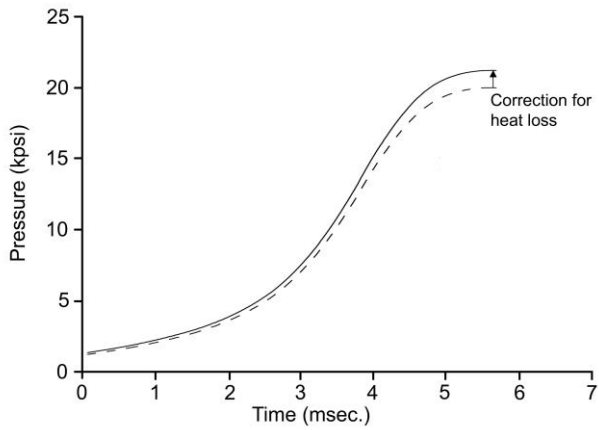

Fig. 4.9 *Correcting the pressures for heat loss*

With the Pressure vs Time trace corrected for heat loss, this can now be differentiated by finding the slope at each point on the trace.

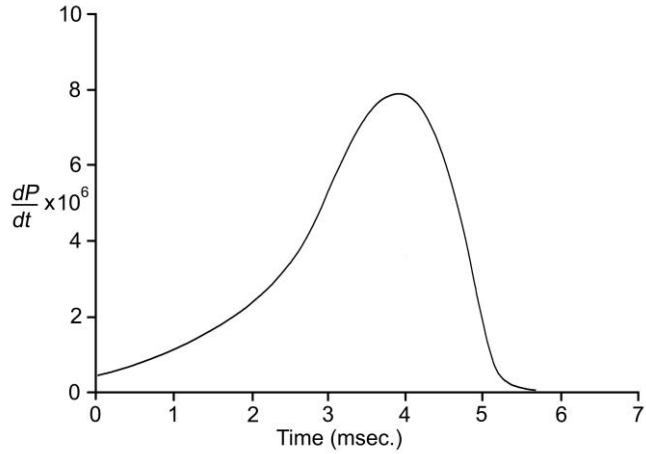

Fig. 4.10 *Rate of change of pressure with time*

With Pressure vs Time, and dP/dt vs Time, it is now possible to plot dP/dt vs Pressure.

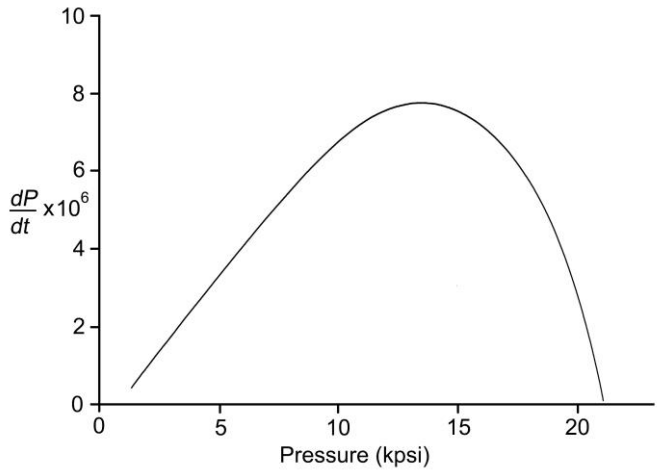

Fig. 4.11 *Rate of change of pressure as a function of pressure*

The trick now is to realise that the maximum pressure P_{Max} occurs when the charge is all burnt at Z = 1. So now re-plot Fig. 4.11 as dP/dt vs P/P_{Max}

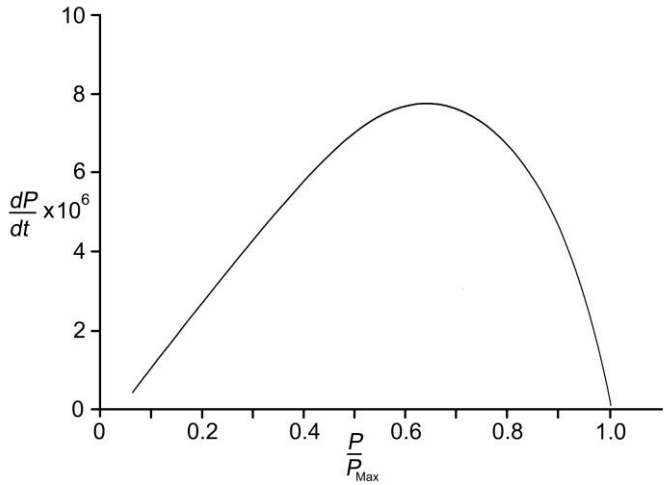

Fig. 4.12 *Rate of change of pressure as a function of* P/P_{Max}

P/P_{Max} can be related to Z by noting that at any given time, the free chamber volume into which the gasses can expand is given by the volume of the empty chamber, minus the volume of the unburnt propellant, minus the volume of the burnt propellant gasses.

$$\text{Free Volume} = V - (1 - Z)\frac{C}{\rho} - Z\eta C \qquad 4.13$$

The Pressure at any time is then,

$$P = \frac{FCZ}{V - (1 - Z)\frac{C}{\rho} - Z\eta C} \qquad 4.14$$

Dividing top and bottom by V, Eqn. 4.14 can be rewritten in terms of loading density.

$$P = \frac{F\Delta Z}{1 - (1 - Z)\frac{\Delta}{\rho} - Z\eta\Delta} \qquad 4.15$$

From Eqn. 4.3 when Z = 1, $F\Delta = P_{Max}(1 - \eta\Delta)$ and then,

$$\frac{P}{P_{Max}} = \frac{Z(1 - \eta\Delta)}{\left[1 - \frac{\Delta}{\rho} - Z\Delta\left(\eta - \frac{1}{\rho}\right)\right]} \qquad 4.16$$

In Fig. 4.13, P/P_{Max} is plotted against Z for a worst case scenario of a loading density with value 0.02 lb/in^3 it can be seen that it only deviates slightly from a straight line with a slope of 1. It is reasonable to conclude that,

$$\frac{d}{dZ}\left(\frac{P}{P_{Max}}\right) \approx 1 \qquad 4.17$$

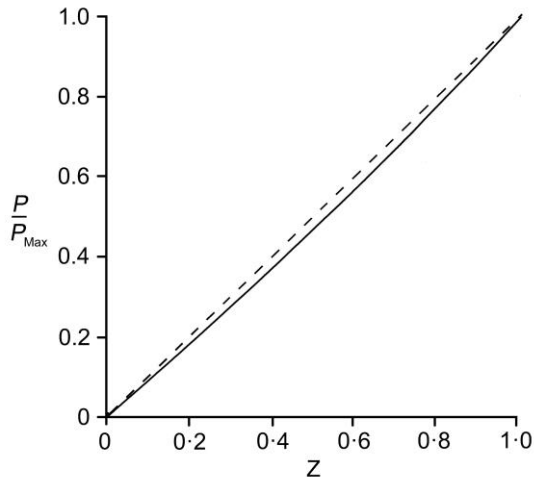

Fig. 4.13 *Plot of* P/P_{Max} *against Z showing* $Z \simeq P/P_{Max}$

Recalling now Eqn. 4.9,

$$\frac{dZ}{dt} = \frac{\text{Area}_Z\ \beta P^{\alpha}}{\text{Volume}} \qquad 4.9$$

$$\frac{dZ}{dt} = \frac{d\left(P/P_{Max}\right)}{dt} \bullet \frac{dZ}{d\left(P/P_{Max}\right)} \quad \rightarrow \quad \frac{d\left(P/P_{Max}\right)}{dt} = \frac{\text{Area}_Z\ \beta P^{\alpha}}{\text{Volume}} \qquad 4.18$$

or,

$$\frac{1}{P_{\text{Max}}}\frac{dP}{dt} = \frac{\text{Area}_Z\,\beta P^{\alpha}}{\text{Volume}} \tag{4.19}$$

or,

$$\frac{1}{P_{\text{Max}}}\frac{dP}{dt}\frac{\text{Volume}}{\text{Area}_Z} = \beta P^{\alpha} \tag{4.20}$$

All the information for the left hand side of Eqn. 4.21 can be measured. Thus the burning rate β and the exponent α can be found by plotting $\log G$ vs $\log P$ where,

$$G = \frac{1}{P_{\text{Max}}}\frac{dP}{dt}\frac{\text{Volume}}{\text{Area}_Z} \tag{4.21}$$

and,

$$\log G = \alpha \log P + \log \beta \tag{4.22}$$

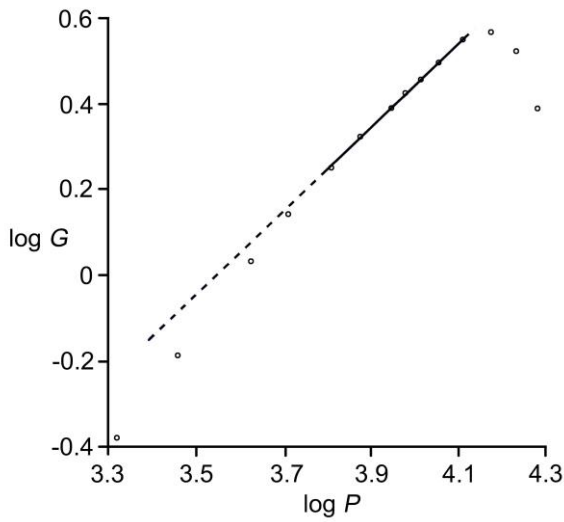

Fig. 4.14 *Plot of log G vs log P to find the burning rate coefficient and the pressure exponent.*

Note that careful interpretation is needed. For the middle part of the plot, where the propellant is not affected by the deterrent coating, the slope of log G against log P is linear and it is unity ($\alpha = 1$). The burning rate coefficient β is readily determined to be

about 2.8 x 10^{-4} in./sec./psi. For the earlier part of the plot, the slope is not linear and reflects how the burning rate coefficient is effectively increasing as the deterrent affected outer layers are burnt away. In the later part of the plot, the kernel disintegrates into slivers and the assumptions for the kernel geometry in Eqn. 4.22 are no longer valid.

§ 4.8 *Dynamic vivacity – the general case*

It is convenient to rewrite the burning rate βP^{α} as $\beta_P P$ where β_P is now not invariant with pressure. This function could be $\beta_P = \left(\beta P^{\alpha-1}\right)$ to recover the Vieille equation, for example, but it allows the possibility of any other function of pressure for the burning rate coefficient. Now, Eqn. 4.19 can be re-written as,

$$\frac{1}{P_{\text{Max}}}\frac{dP}{dt} = \frac{\text{Area}_{\text{Z}}\,\beta_{\text{P}}\,P}{\text{Volume}} \qquad 4.23$$

Dividing through by pressure gives,

$$\frac{1}{P\cdot P_{\text{Max}}}\frac{dP}{dt} = \frac{\text{Area}_{\text{Z}}\,\beta_{\text{P}}}{\text{Volume}} = \Lambda_{\text{Z, P}} \qquad 4.24$$

where $\Lambda_{\text{Z, P}}$ is the *dynamic vivacity* of the propellant powder and is the rate at which the propellant is turned into propellant gasses per unit of pressure. Note that here, the dynamic vivacity is a function of Z, the amount of gas burnt, and also of pressure.

From Eqn. 4.9 the rate of gas production can now be written as,

$$\frac{dZ}{dt} = \frac{\text{Area}_{\text{Z}}\,\beta_{\text{P}}\,P}{\text{Volume}} = \left[\frac{1}{P\cdot P_{\text{Max}}}\frac{dP}{dt}\right]P = \Lambda_{\text{Z,P}}\,P \qquad 4.25$$

The dynamic vivacity $\Lambda_{\text{Z, P}}$ can be determined experimentally by firing a closed bomb over a range of different loading densities, so that for any given Z, the value of Λ can be plotted for a range of pressures. A three dimensional plot can then be created of dynamic vivacity as a function of Z and *P*. For a numerical internal ballistics system, the value of Z and *P* at any given time will be known, and so an appropriate value of $\Lambda_{\text{Z, P}}$ can be extracted from this three dimensional plot to solve Eqn. 4.25.

§ 4.9 *Effect of loading density on burning rate measurements*

In practice, it is found that for most propellants, burning rates and dynamic vivacities as determined by closed bomb tests are not significantly affected by changes in the loading density [31].

Schmitz showed experimentally [30] that,

$$\int_{t}^{t_{P_{max}}} P\,dt = \text{constant} \qquad 4.26$$

where the constant is independent of the loading density. It is quite easy to show in a numerical simulation that Schmitz's law is true if, and only if, the pressure exponent $\alpha = 1$.

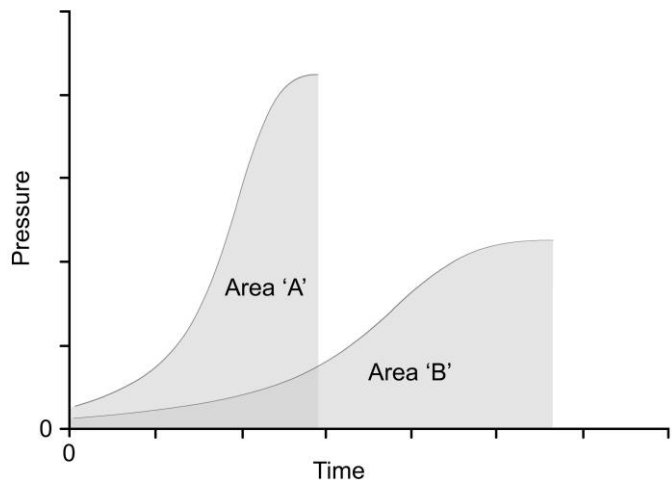

Fig. 4.16 *Schmitz law. The area under the pressure time curve to the point of maximum pressure in invariant with loading density. The areas for firings* 'A' *and* 'B' *are the same, despite the loading density in the case of* 'A' *being twice that for* 'B'. *This is only true if* $\alpha = 1$.

§ 4.10 *Dynamic vivacity – where the pressure exponent α is unity*

If $\alpha = 1$ then it follows that the ratio $\frac{1}{P \cdot P_{Max}} \frac{dP}{dt}$ in Eqn. 4.25 will also be invariant with loading density. Where $0.9 < \alpha < 1.1$ the error introduced would seem to be within experimental error. In consequence, there is no 'preferred' loading density in closed bomb tests, other than for the practical reasons that if the loading density is too low, adjusting for heat loss to the chamber walls becomes difficult and if the loading density is too high, the pressure integrity of the chamber could be compromised.

If $\alpha = 1$ then Eqn. 4.25 can now be written as,

$$\frac{dZ}{dt} = \left[\frac{1}{P \cdot P_{Max}} \frac{dP}{dt} \right] P = \Lambda_Z P \qquad 4.27$$

where the dynamic vivacity is now only a function of Z, the amount of powder burnt, and is invariant with pressure.

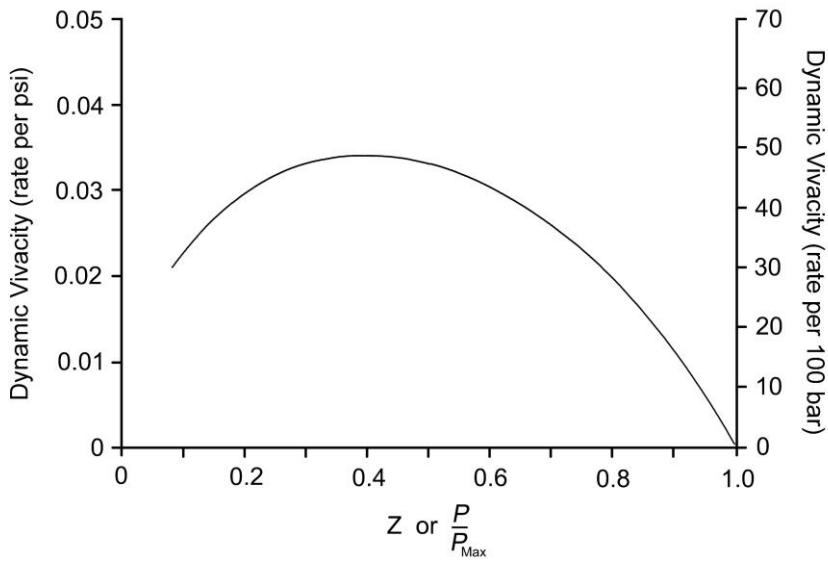

Fig. 4.15 *Plot of dynamic vivacity against* Z. *Dynamic vivacity is commonly quoted as a rate per hundred bar.*

Fig. 4.15 above gives the dynamic vivacity for the closed bomb pressure-time curve analysed in the discussion above. Note that when using dynamic vivacity, no knowledge of the powder kernel geometry or the burning rate coefficient is required.

These days, most small-arms propellant powder manufacturers publish the burning characteristics of their powders as a dynamic vivacity plot, rather than as a burning rate coefficient. Given that most small-arms propellant powders are modified by deterrents on the kernel surface to enhance the progressive qualities of the powder, it would be difficult to describe the burning rate of the powder by a burning rate coefficient. But the use of dynamic vivacity naturally encompasses the effects of deterrents.

In a numerical internal ballistics system, the value of Z is known at any stage of the computation and so it convenient to use the dynamic vivacity for the given value of Z to calculate the gas production rate. The experimental plot for dynamic vivacity as a function of Z is not a simple function, but in a numerical system the data can (for example) be stored as an array of spot values and then the dynamic vivacity for any given value of Z is determined by interpolation (see Appendix 1).

§ 4.11 *Anomalous enhanced vivacity at low Z due to progressive powder ignition*

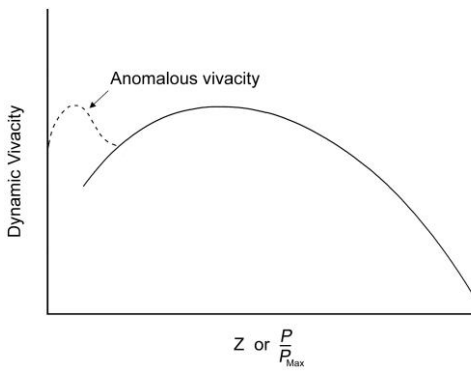

Fig. 4.16 *Anomalously high dynamic vivacity at low Z caused by uneven powder ignition*

It is rarely the case that all the powder kernels in a closed bomb test will ignite at the same time and burn at the same rate for the same period. However, the consequence of progressive powder kernel ignition, where the number of burning powder kernels increases progressively with time, is particularly noticeable in creating an anomalously high value of dynamic vivacity for low Z values. This is because the rate of increase of gas generation is higher if powder kernel ignition is progressive rather than simultaneous. This frequently means that the dynamic vivacity data for $Z < 0.1$ (or even $Z < 0.2$) is discarded.

§ 4.12 *Reduced dynamic vivacity at high* Z

If the burning rate coefficient β is invariant with Z and with pressure, as might be expected for any unmodified propellant powder, then from Eqn. 4.25 it would be expected that the dynamic vivacity should be a function of geometric form alone. Common kernel shapes would be expected to follow the forms in Fig. 4.8, for example. Neutral forms, such as flake or cylinder with one perforation, would be expected to be reasonably constant for all Z. However, practical measurements of dynamic vivacity invariably show a steady decline to zero as $Z \rightarrow 1$, as in Fig. 4.15. The explanation is that the form of the powder kernel does not retain its integrity right up to the moment when the web thickness *w* reaches zero. The kernel starts to break up into slivers somewhat earlier, particularly for perforated kernels where the gas pressure inside the perforation breaks the kernel up well before its theoretical point of slivering.

The slivers that remain after the kernel has broken up will generally have a much more divergent shape than the original kernel and, as shown in Fig. 4.8, the dynamic vivacity of these divergent shapes will be expected to tend to zero as $Z \rightarrow 1$.

§ 4.12 *Correction to closed bomb data when using it for a gun*

Generally, it is found that closed bomb burning rates and vivacities understate the values experienced when the same propellant powder is used in a gun. This is generally attributed to *erosive burning* of the propellent, which is an increase in burning rate due to the propellant gasses flowing over the surface of the propellant granules in a gun, rather than the gasses being static as in a closed bomb.

An erosive 'fudge factor' commonly added to the burning rate β determined in a closed bomb is 0.00036 multiplied by the instantaneous projectile velocity in inches per second. This typically increases the burning rate at peak pressure in a gun by about 10%.

Nomenclature

C = charge weight: pounds (7000 grains – one lb)
F = Force or impetus of the propellant: inch-pounds/inch^3.
P = gas pressure: pounds/inch^2 or psi.
P_{Max} = maximum gas pressure: pounds/inch^2 or psi.
t = time: seconds
V = volume: inch^3
V_0 = the free space behind the projectile when loaded with propellant: inch^3
w = web thickness: inches
y = the amount by which the burning surface has regressed: inches
Z = the fractional amount of charge burnt: dimensionless
α = the pressure exponent in Vieille's equation.
β = the burning rate of the powder: inches/sec/psi.
γ = the ratio of specific heats for the propellant gasses:
ρ = the density of the unburnt propellant: pounds/inch^3
η = the covolume of the propellant gasses: inch^3/pound
Λ = the vivacity of the propellant: rate per unit pressure. (often quoted /100 bar/sec.)

References

[1] T. J. Hayes, "Elements of Ordnance", John Wiley & Sons, New York (1938)

[2] M. Koshi, "Smoke Generation in Black Powder Combustion" Sci. Tech. Energetic Materials, Vol. 79, No. 3, pp. 59-69 (2018)

[3] R. A. Sasse, "A Comprehensive Review of Black Powder" Ballistics Research Laboratory Research Report BRL-TR-2630, January (1985)

[4] J.D. Blackwood and F.P. Bowden, "The Initiation, Burning and Thermal Decomposition of Black Powder" Proceedings of the Royal Society, Series A, Vol. 213, pp 285-306, (1952)

[5] C. Campbell and G. Weingarten, "A Thermoanalytical study of the Ignition and Combustion Reactions of Black Powder" Transactions of the Faraday Society, Vol 55, pp 2221-2228 (1959)

[6] L. Bruff, "Textbook of Ordnance and Gunnery" John Wiley & Sons, 2nd Ed. p-19 (1903)

[7] M. E. Brown and R. A. Rugunanan, "A Temperature Profile Study of Black Powder and its Constituent Binary Mixtures" Propellants, Explosives, Pyrotechnics, Vol. 14, pp. 16-75 (1989)

[8] E. Freedman, "Gun Propulsion Technology" Progress in Astronautics and Aeronautics, Vol. 109, Ed. Ludwig Steifel, p-128, (1988)

[9] C. S. Robinson, "Thermodynamics of Firearms", McGraw-Hill, New York, p. 29 (1943)

[10] G. Piobert, "Traité d' Artillerie", (1839)

[11] P. Vieille, "Mémorial des Poudre et Salpétres", Vol. 6, pp. 256-391 (1893)

[12] *cf.* Berthelot "Sur la Force des Matieres Explosives" Vol. 1, p. 85 (1883)

[13] B. Grollman and C. Nelson, "Burning Rates of Standard Army Propellants in Strand Burner and Closed Chamber Tests" USA Ballistic Research Laboratory, Report No. 2775 (1977)

[14] N. Kubota et al, "The Mechanism of Super Rate Burning of Catalysed Double Based Propellants" Office of Naval Research, Report AD-763-786 (1973)

[15] J. Corner, “The Theory of the Interior Ballistics of Guns”, John Wiley & Sons, New York, Chapter 2 (1950)

[16] “Internal Ballistics”, Edited by F.R.W. Hunt, Pub. Philosophical Library of New York, Chapter XIII (1951)

[17] D-H Han, Y-L Yoo and H-G Sung, “An Analysis of the Different Flow Characteristics of a Closed Bomb Test in Cylindrical and Spherical Closed Vessels”, International Journal of Aeronautical and Space Sciences, Vol. 20, Issue 1, pp150-156 (2019)

[18] J. Petavel, “The Pressure of Explosions: Experiments on Solid and Gaseous Explosives”, Philosophical Transactions A, Vol. 205, pp 357-398 (1905)

[19] Kingenberg

[20] A. Crowe and W. Grimshaw, “On the Equation of State of Propellant Gasses”, Philosophical Transactions A, Vol. 230, pp 39-73 (1931)

[21] R. Kent and J. Vinti, “Cooling Corrections for Closed Chamber Firings”, Ballistics Research Laboratory, Report 281, (1942)

[22] U. Kulkarni and S. Naik, “Modelling of Heat Loss in Closed Vessels During Propellant Burning”, Defence Science Journal, Vol. 50, No. 4, pp 401-409 (2000)

[23] S. Dean, J. Morris and J. Gottfried, “Heat Loss in a Micro-Combustion Chamber”, Army Research Laboratory, Report ARL-TN-0908 (2018)

[24] J. Corner, “Theory of Interior Ballistics of Guns”, Pub. John Wiley & Sons, p. 88 (1950)

[25] P. Charbonnier, “Balistique Intérior”, Dion, Paris (1908)

[26] “Internal Ballistics”, Edited by F.R.W. Hunt, Pub. Philosophical Library of New York, Chapter 4, (1951)

[27] J. Petavel, “The Pressure of Explosions: Experiments on Solid and Gaseous Explosives”, Philosophical Transactions A, Vol. 205, pp 357-398 (1905)

[28] “Textbook for Smallarms”, Pub. The War Department, (1929)

[29] A. Webster and L. Thompson, "A New Instrument for Measuring Pressure in Guns", Proceedings of the National Academy of Sciences, Vol. 5, pp 259-263 (1919)

[30] M.E. Serabryakov, "Interior Ballistics", Air Technical Intelligence Translation, Wright-Patterson Air Fore Base, Ohio, pages 119-122, (1968)

[31] P. Mehta et al, "Effect of Loading Densities in Closed Vessel Tests on the Burning Rate of a Propelling Charge", Defence Science Journal, Vol. 65, pp 126-130, (2015)